Techno-economic comparative assessment of the ultrasound, electrostatic and microwave supported coalescence of binary water droplets in crude oil

Idowu Adeyemi [b], Mahmoud Meribout [a],[*], Lyes Khezzar [c], Nabil Kharoua [c], Khalid AlHammadi [a]

[a] Department of Electrical Engineering and Computer Science, Khalifa University, P.O. Box 127788, Abu Dhabi, United Arab Emirates
[b] Department of Mechanical Engineering, Khalifa University, P.O. Box 127788, Abu Dhabi, United Arab Emirates
[c] Ecole Nationale Polytechnique de Constantine, Constantine, Algeria

ARTICLE INFO

ABSTRACT

In this study, comparative assessment of the technical performance, energy usage and economic impact of ultrasound, electrostatics and microwave on the coalescence of binary water droplets in crude oil was conducted. The effect of different oil properties such as crude oil viscosity (10.6–106 mPa s) and interfacial tension (IFT) (20–250 mN/m) on the coalescence time and energy consumption was examined. In addition, operation conditions such as inlet emulsion flow velocity (10–100 mm/s), electric field type, ultrasound frequency and applied voltage amplitude (0–30 kV) were evaluated. The numerical models showed good agreement with experimental findings in the literature. Moreover, the process time of the dewatering process increased with rising inlet flow velocities. The elevation of the coalescence time with velocity can be attributed to the increasing effect of flow disturbance, and the reduction of the emulsion residence time. As regards the IFT, the coalescence time reduced as the IFT was increased. This can be associated with the improved stability of emulsions formed at lowered IFT. As the maximum droplet size is directly proportional to the IFT, lowering the IFT reduces the peak diameter of the droplets that are present in the emulsion. Moreover, the coalescence time followed the order: ultrasound < microwave < electrostatics approaches under varying IFT. The coalescence energy increased from ~15 J, ~90 J and ~25 mJ to ~61 J, ~235 J and ~26 mJ for microwave, electrostatics and ultrasound techniques, respectively, as the viscosity was raised from 10.6 to 106 mPa s. Ultrasound coalescence showed significant energy and economic savings in comparison to microwave and electro-coalescence. Hence, ultrasound coalescence would be a potential method for standalone or integrated demulsification over the two other techniques. However, there are indications that beyond a viscosity of 300 mPa s, the effect of ultrasound becomes weak with significant hindrance to droplet movement and accumulation. This analysis provides fundamental insights on the comparative behavior of the three emulsion separation techniques.

1. Introduction

The existence of stable emulsions during oil production and processing continue to pose substantial environmental and economic drawbacks during exploration, transportation and refining. For instance, untreated crude oil emulsions could cause clogging and erosion of transportation pipelines and equipment parts [1,2]. Moreover, the viscosities of water-in-oil emulsions are significantly higher than that of water and crude oil. This results in drops in operation pressure and excessive cost of pumping [3–5]. Likewise, there have been reports of catalyst poisoning due to emulsions during oil refining [6–8]. These emulsions are often produced due to the abundance of water and

turbulence during oil extraction and processing. The aqueous medium originate from immense underground formation water, water drilling and flooding as well as prolonged utilization of oil reservoirs. The water combines with the crude oil which produces stable emulsions under flow turbulence at chokes and constricted pores as well as surface active agents. Due to the prevalence of these emulsions and the associated operational difficulties, numerous evaluation of different methods, parameters and operating conditions for crude oil emulsion dehydration have been conducted [9–20].

The key approaches that have been investigated for the demulsification of oil emulsions are biological [9–11,21–23], chemical [12–15] and physical [16–20] methods. Biological approach usually involves the utilization of certain whole cells or bacterial metabolites such as

---

* Corresponding author.
E-mail address: mahmoud.meribout@ku.ac.ae (M. Meribout).

Nomenclature

IFT	Interfacial tension	Re	Reynolds number
IL	Ionic liquid	We	Weber number
SAGD	Steam assisted gravity drainage	ECS	Electrostatics
PZT	Lead zirconate titanate	MWV	Microwave
D	Electric displacement	USW	Ultrasonic Waves
e	Coupling matrix	V	Applied voltage
S	Strain	Q_m	Monopole domain source
ε_s	Permittivity matrix	p_t	Total pressure
E	Electric field	k_{eq}	Wave number
c_E	Elasticity matrix	ω	Angular frequency
ρ_v	Electric charge density	c	Speed of sound
k_o	Free space wave number	p_b	Background pressure
μ_r	Relative permeability	ε_r	Relative permittivity
Q	Electromagnetic loss	ε_o	Vacuum permittivity
ρ	Density	ε_r''	Relative permittivity losses
c_p	Fluid thermal conductivity	μ_r''	Relative permeability losses
μ	Viscosity	H	Magnetic field intensity
F_σ	Interfacial tension	F_{ext}	External force
ϕ	Phase field dimensionless function	V_f	Volume fraction
ε	Level thickness	h	Mesh element size
We_{cr}	Critical Weber number	t	Time
AC	Alternating current	d_f	Final droplet diameter
DC	Direct current	d_i	Starting droplet diameter
		DEWA	Dubai Electricity and Water Authority

Achromobacter, Bacillus and Alcaligenes species for oil dehydration. Although microbial dewatering provides enhanced environmental and energy savings benefits, they are hampered by several technical challenges. The usage of microbes often encounters challenges such as prohibitive production cost, which becomes more significant with increased scale of operation [21]. In addition, the biological process can be severely limited by operating conditions such as elevated temperature, varying pH etc. [9–11]. Chemical demulsification provides advantages with flexibility and high separation efficiency. However, chemical demulsifiers are hindered by their detrimental impact on human health and environment as well as the significant cost requirements. Although novel chemical demulsifiers have been developed, there remains significant challenges that need to be addressed. For instance, ionic liquids (ILs) and deep eutectic solvents demulsifiers usually have significant viscosities which could reach 85,000 mPa s [24–26] and several ILs remain toxic to micro-organism and aquatic life [27,28]. The increased viscosity of ILs could result in prohibitive pumping costs. Moreover, the utilization of nanoparticles has potential health effects [29]. Due to their very small size, nanoparticles could be inhaled and cause heart problems, lung inflammation and damages [30]. Hence, their usage needs to be carefully controlled or minimized to avoid these adverse health impacts.

Consequently, there is a need for the development of potential substitutes to chemical and biological demulsifiers. Physical dehydration techniques are important solution portfolio with prospects for alleviating the environmental, technical and economic challenges faced by other methods. Because of their physical separation mechanisms, the environmental impact and human health influences are relatively minimal in comparison to chemical methods. Moreover, physical methods could be used in combination with chemical dewatering to lower the usage and environmental degradation associated with surfactants. Amongst the physical approaches that have been investigated, ultrasound, electrostatic and microwave supported oil emulsion coalescence are the three main demulsification techniques. Ultrasound, electrostatic and microwave supported coalescence provide enhancements over chemical and biological approaches. Hence, several studies have evaluated their usage for demulsification of crude oil emulsions [16–19].

Ultrasound has been commonly used for the demulsification of crude oil emulsions because of their enhanced efficiencies, simple design and improved economic benefits [9,31,32]. The main drivers during the ultrasound emulsification of oil emulsions are primary and secondary acoustic forces, van der Waal forces, net buoyancy-gravitational forces and hydrodynamic interactions [33–36]. As regards electro-coalescence, it is widely utilized for the dehydration of emulsions in oil refineries [37–39]. The application of electric fields to these emulsions provides improvements in droplet approach through di-electrophoresis, electrophoresis and dipolar attractions [39,40]. Subsequently, the coalescence between droplets in the continuous phase is promoted. Although the usage of electric field is usually restricted to low water fractions [20], there are reports that indicate the feasibility of utilizing alternating current fields for the demulsification of oil emulsions [39]. On microwave coalescence, numerous reports have highlighted their viability over traditional thermal and RF coalescence method [41–43]. Owing to the selective heating of microwaves, less energy requirements and better coalescence performance are achievable. In addition, microwave is suitable for oil emulsions with high water concentrations [20,44]. Even with the developments witnessed with these three physical demulsification methods, their comparative evaluation under similar conditions is rare.

The comparison of these three methods is critical due to their significance to the demulsification portfolio. Although some studies have focused on the assessment of standalone and integrated demulsification approaches, there is a need for further evaluation of these techniques. There have been reports on microwave-electro-coalescence [45,50], microwave-ultrasound coalescence [49], ultrasound-chemical [47,48], ultrasound-electro-coalescence [56], microwave-chemical [54,55] and other combinations [46,51–53]. For instance, in their study, Yi et al. [48] assessed the demulsification of water in crude oil emulsion with natural sedimentation, ultrasound, chemical, and sono-chemical methods. The Daqing crude oil contained preliminary water fraction of ~0.25. The dehydration approaches were examined at 40, 60 and 70 °C. Furthermore, the ultrasound probe had a resonance frequency of 20 kHz and a maximal power of 150 W. Surfactant Protein (SP) of concentration of 0.25 g/L was used for the chemical separation method.

They observed that the demulsification efficiency of the techniques followed the order: Natural sedimentation < Ultrasound < Chemical < Ultrasonic Chemical at the three temperatures studied. For instance, the dewatering efficiencies at 60 °C were ~4.82%, ~11%, ~18.5% and ~33.5% for natural sedimentation, ultrasound, chemical and sono-chemical methods, respectively. Similar performance trend was reported by Xu et al. [57] in their study on the demulsification of steam assisted gravity drainage (SAGD) crude oil emulsion. They showed that chemical demulsification provided better separation efficiency compared to ultrasound at 40, 50, 60 and 70 °C. In a different study, Yang et al. [47] conducted a comparative assessment of crude oil demulsification performance for ultrasonic chemical and thermal chemical methods. The experiments were conducted at US frequency and power of 40 kHz and 100 W, respectively. In addition, temperatures of 55, 65, and 75 °C were used. The crude oil was obtained from Dagang oil field with water content of 35% on a volume by volume basis. Surfactant of polyester type was utilized at 50 mg/L for the chemical separation. They highlighted that the ultrasonic chemical methods provided enhanced performance compared to the thermal chemical methods. At 55 °C, separation efficiencies of 79.2% and 48.2% were attained for the sono-chemical and thermochemical methods, respectively. However, the differences in the demulsification performance for the two methods was reduced drastically with rising temperature. The performance decreased to a margin of 2.7% and 1.2% at 65 and 75 °C, respectively. In another study, Parvasi et al. [49] stated that microwave showed significantly improved demulsification compared to ultrasound coalescence at elevated crude oil viscosity based on a trajectory model. However, the study is not comprehensive for different oil properties, and separation under continuous flow was not considered. In other studies, the improvements provided by microwave over natural sedimentation [20] and conventional heating methods [45,46] have been reported.

Based on the assessment of the reported literature, techno-economic comparative assessment of ultrasound, microwave and electro-coalescence under similar conditions had not been conducted. Hence, in this study, the comparative analysis of the technical performance, energy consumption and economic assessment of ultrasound, electrostatic and microwave enhanced coalescence of binary water droplets in crude oil was conducted. The effect of different oil properties such as crude oil viscosity (10.6–106 mPa s) and interfacial tension (20–250 mN/m) on the coalescence time and energy consumption was examined. In addition, operation conditions such as inlet emulsion flow velocity (10–100 mm/s), electric field type, ultrasound frequency and applied voltage amplitude (0–30 kV) were assessed. This analysis provides fundamental insights on the behavior of the three emulsion separation techniques under different crude oil properties and process conditions.

2. Methodology

The coalescence of binary droplets of water in crude oil phase was evaluated under continuous flow conditions. Three different demulsification approaches were investigated numerically in COMSOL 6.0. The methods, which includes ultrasound, electrostatics and microwave, were examined under similar emulsion properties and process conditions. The emulsion consists of two water droplets in crude oil. The water droplets have diameters of 1.27 and 1.52×10^{-3} mm, and an inclination angle of 14.93° to the vertical axis. The assessment was conducted in a pipe of diameter of 50.8 mm, and cross section length of 50.8 mm. The model geometry was discretized into meshes which is composed of triangular elements with different mesh sizes. This allows for the analysis of the independency of the mesh on the output performance of the model.

2.1. Ultrasound modeling

The model geometry consists of the piezoelectric transducer which is mounted on a pipe of diameter of 50.8 mm (Fig. 1). The pipe contains emulsion of binary water droplets in crude oil, and the transducer material utilized is lead zirconate titanate (PZT). PZTs are technically favorable in demulsification processes due to their relatively high piezoelectric coefficient (~600 pC/N). The US transducer has a diameter of 25.4 mm and height of 25.4 mm, and operates at a resonance frequency of 26.04 kHz. This frequency provided the best performance for the ultrasound coalescence. For example, the coalescence time of the binary droplets at 26.04 kHz was 30 ms. However, at 20 kHz and 35 kHz, the process times were 84 ms and 76.5 ms, respectively. The resonance frequency was selected based on Eigen value analysis of the PZT transducer. It was modeled by coupling the electrostatics and solid mechanics physics, based on the principle of piezoelectric effect. The acoustic propagation in the oil emulsion was described with the pressure acoustics, frequency domain physics. The governing equation for the piezoelectric transducer is based on the stress-charge constitutive (Eqs. (1) and (2)) and Gauss (Eq. (3)) equations. The electric displacement (D) is described as [58]:
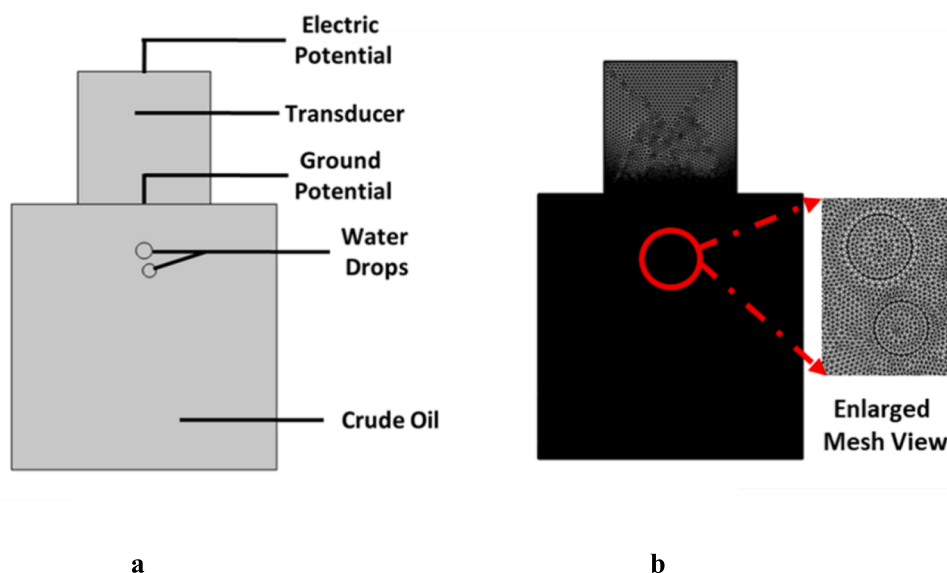
Fig. 1. a. Ultrasound coalescence model description b. Mesh utilized for droplet coalescence.

$$D = eS + \varepsilon_s E \qquad (1)$$

where e is coupling matrix, S is strain, ε_s is permittivity matrix and E is the electric field.

The piezoelectric material stress (T) is defined as [58]:

$$T = c_E S - e^T E \qquad (2)$$

where T is the stress, c_E is elasticity matrix and e^T is the coupling matrix transpose.

The Gauss law is represented as [58]:

$$\nabla \bullet D = \rho_v \qquad (3)$$

where ρ_v is the electric charge density.

The electric field (E) is defined as follows [58]:

$$E = -\nabla V \qquad (4)$$

where V is the applied voltage.

The pressure acoustic was used to propagate the ultrasonic wave in the emulsion, and it is defined as [58]:

$$\nabla \bullet \left(\frac{-1}{\rho} (\nabla p_t - q_d) \right) - \frac{k_{eq}^2 p_t}{\rho} = Q_m \qquad (5)$$

where Q_m is the monopole domain source, ρ is the piezoelectric domain density, q_d is the monopole domain source, and p_t is the total pressure. k_{eq} is the wave number consisting of the ordinary wave number k, the azimuthal wave number and the out of plane wave number k_z. The wave number (k_{eq}) is defined as [58]:

$$k_{eq}^2 = \left(\frac{\omega}{c} \right)^2 - k_z^2 \qquad (6)$$

where ω is the angular frequency and c is the speed of sound.

The total pressure (p_t) is defined as follows [58]:

$$p_t = p + p_b \qquad (7)$$

where p_b is the background pressure.

2.2. Electrostatics modeling

The model geometry consists of the electric and ground potential electrodes at the top and bottom of the emulsion compartment, respectively (Fig. 2). The electrodes (length = 25.4 mm) were described through the electrostatics physics. Based on the applied potentials, electrostatic force propagates through the crude oil emulsion. This force provides significant influence on the droplet coalescence and emulsion flow dynamics. The electrostatic force (F_{ec}) is represented as [59]:

$$F_{ec} = \nabla \bullet \tau \qquad (8)$$

where τ is the Maxwell stress tensor, which is defined as [59]:

$$\tau = E D^T - \frac{(E \bullet D) I}{2} \qquad (9)$$

where E is the electric field, D is the electric displacement field, D^T is the transpose matrix of the electric displacement field and I is the identity matrix.

The electric field (E) is defined as [59]:

$$E = -\nabla V \qquad (10)$$

where V is the applied voltage.

The electric displacement field (D) is defined as [59]:

$$D = \varepsilon_r \varepsilon_o E \qquad (11)$$

where ε_r is the relative permittivity and ε_o is the vacuum permittivity.

The electric field signal utilized for the coalescence process is the sinusoidal waveform. This provides enhanced technical performance in comparison to different waveforms such as triangular and saw-tooth signals. For instance, sinusoidal field provided coalescence in 135 ms, but triangular waveform required a process time of 140 ms. Based on the assessment of 0–30 kV, the energy consumption showed an increasing–decreasing trend with a maximum at 20 kV. Hence, the applied voltage used in this study is generally lower than 20 kV due to this peak energy requirement for coalescence.

2.3. Microwave modeling

The model geometry consists of the microwave inlet and outlet ports,

a **b**
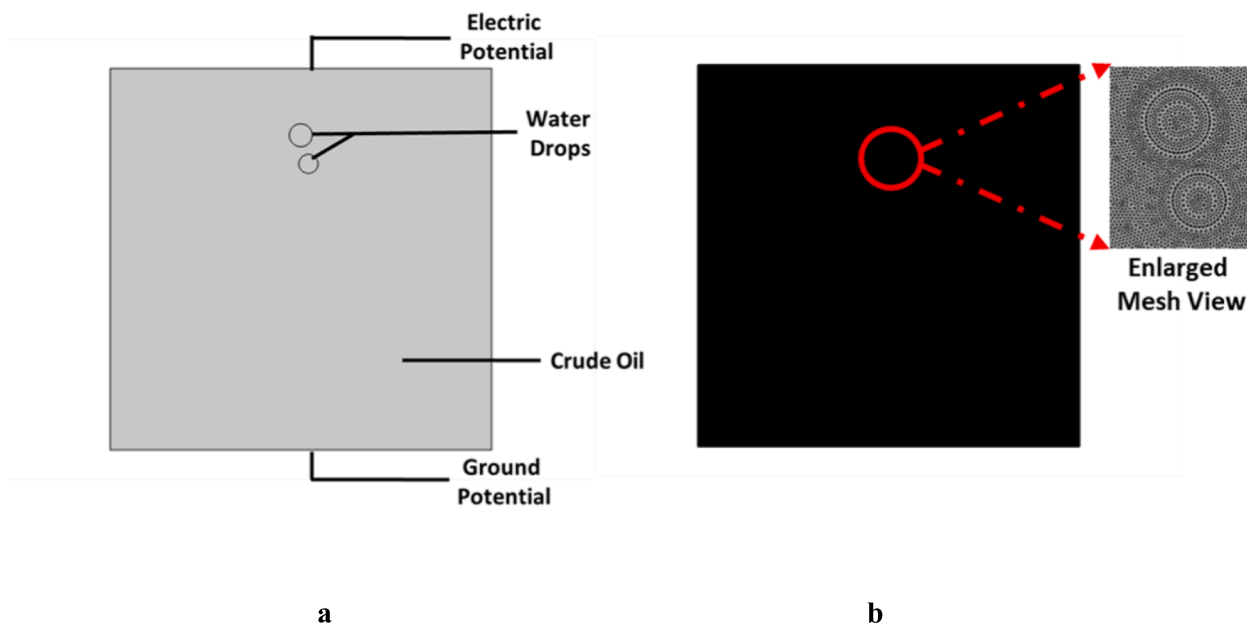
Fig. 2. a. Electro-coalescence model description b. Mesh utilized for droplet coalescence.

copper walls and the crude oil emulsion surrounded by air (Fig. 3). The microwave is channeled into the oil emulsion from the inlet port through air. Thereafter, the microwave exits through the outlet port. Copper walls were used because of their low absorptivity to microwaves. The microwave simulation includes the electromagnetic waves (frequency domain) and heat transfer physics. Furthermore, the electromagnetic heating and non-isothermal flow multi-physics were utilized to integrate the model physics. The introduced microwave at the inlet port was defined based on the wave equation as follows [60]:

$$\nabla \times \left(\mu_r^{-1} \nabla \times E \right) - k_o^2 \left(\varepsilon_r - \frac{j\sigma}{\omega \varepsilon_o} \right) E = 0 \qquad (12)$$

where k_o is the free space wave number, μ_r is the relative permeability, ∇ is the Del function, E is the electric field intensity, ε_r is the relative permittivity, ε_o is the vacuum permittivity, ω is the angular frequency and σ is the electrical conductivity.

Due to the electromagnetic field propagation, there are losses related to the electric field, magnetic field dipoles and conduction heat. The electromagnetic losses include the losses due to the electric field dipoles which is defined as [60]:

$$Q_{Edipole} = \frac{1}{2}\varepsilon_r'' \omega E \bullet E^* \qquad (13)$$

where ε_r'' is the relative permittivity losses.

The losses due to the magnetic field dipoles is defined as [60]:

$$Q_{Hdipole} = \frac{1}{2}\mu_r'' \omega H \bullet H^* \qquad (14)$$

where μ_r'' is the relative permeability losses and H is the magnetic field intensity.

The losses due to the conduction heat is defined as [60]:

$$Q_{cond} = \frac{1}{2}\sigma E \bullet E^* \qquad (15)$$

where Q_{cond} is the conduction heat.

The total electromagnetic losses (Q) is the aggregate of the losses and it is represented as [60]:

$$Q = Q_{cond} + Q_{Edipole} + Q_{Hdipole} \qquad (16)$$

The cumulative heat losses translate into the electromagnetic heating source, and it is incorporated in the heat transfer equation as follows [60]:

$$\rho c_p \frac{\partial T}{\partial t} + \nabla \bullet (-k\nabla T) = Q \qquad (17)$$

where ρ is the fluid density, c_p is the fluid heat capacity, k is the fluid thermal conductivity and T is the temperature.

The heat transfer provides changes in the properties of the emulsion such as viscosity and surface tension. Hence, the modified emulsion properties influence the nature of the coalescence dynamics. Microwave frequency and power of 2.45 GHz and 254 W, respectively, were utilized for the coalescence. Although microwave frequency band is broad (0.3–300 GHz), heating applications are limited to 0.92 and 2.45 GHz. However, the maximum electric field and heating capacity at 0.92 GHz is relatively small. Similar conditions have been experimentally used for microwave coalescence [19,20,87].

2.4. Flow and coalescence dynamics

The emulsion flow and droplet coalescence dynamics is influenced by different techniques through either external force or emulsion properties. The ultrasound and electro-coalescence were incorporated into the fluid dynamics through external forces, and the microwave model was implemented with modified emulsion properties. The coalescence model includes the mass conservation in the form of continuity equation (Eq. (18)). Moreover, the momentum conservation was implemented based on the incompressible form of the Navier-Stokes equations (Eq. (19)) [61].

$$\nabla \bullet u = 0 \qquad (18)$$

$$\rho \frac{\partial u}{\partial t} + \rho(u.\nabla)u = -\nabla p + \left(\mu \left(\nabla u + \nabla u^T \right) \right) + F_\sigma + F_{ext} + \rho g \qquad (19)$$

where F_{ext} is the external force, μ is the emulsion viscosity, ρ is the emulsion density, F_σ is the interfacial tension, u is the fluid velocity vector, g is gravity, t is the time, p is the pressure.

The emulsion density is defined as follows [61]:
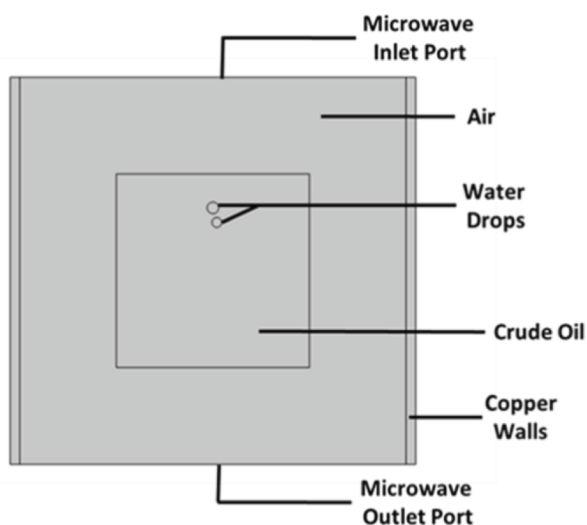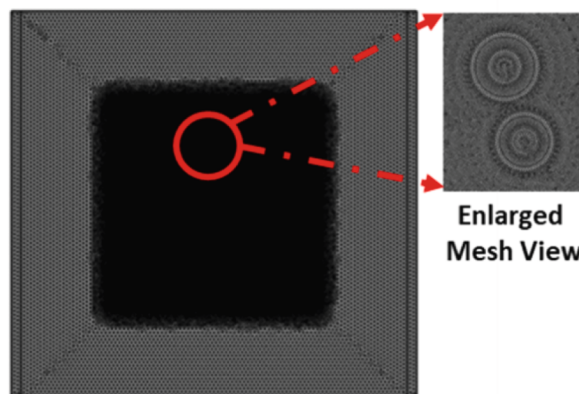
Fig. 3. a. Microwave coalescence model description b. Mesh utilized for droplet coalescence.

$$\rho = \rho_w + (\rho_o - \rho_w)V_f \qquad (20)$$

The emulsion viscosity is represented as follows [61]:

$$\mu = \mu_w + (\mu_o - \mu_w)V_f \qquad (21)$$

where ρ_o is the crude oil density, ρ_w is the water density, μ_o is the crude oil viscosity, μ_w is the water viscosity and V_f is the volume fraction.

The volume fraction is described as [61]:

$$V_f = \min\left(\max\left[\frac{1+\phi}{2}, 0\right], 1\right) \qquad (22)$$

where ϕ is a phase field dimensionless function.

The interfacial force is described based on a phase field interface as follows [61]:

$$F_\sigma = \lambda\left(-\nabla^2\phi + \left(\frac{\phi(\phi^2 - 1)}{\varepsilon^2}\right)\right)\nabla\phi \qquad (23)$$

where ε is the level thickness and λ is the mixing energy density.

The phase field dimensionless function (ϕ) and support variable (ψ) are described as below [61]:

$$\frac{\partial\phi}{\partial t} + u.\nabla\phi = \nabla \bullet \frac{\sigma\lambda}{\varepsilon^2}\nabla\psi \qquad (24)$$

$$\psi = -\nabla \bullet \varepsilon^2\nabla\phi + (\phi^2 - 1)\phi + \left(\frac{\varepsilon^2}{\lambda}\right)\frac{\partial f_{ext}}{\partial\phi} \qquad (25)$$

where f_{ext} is the external force.
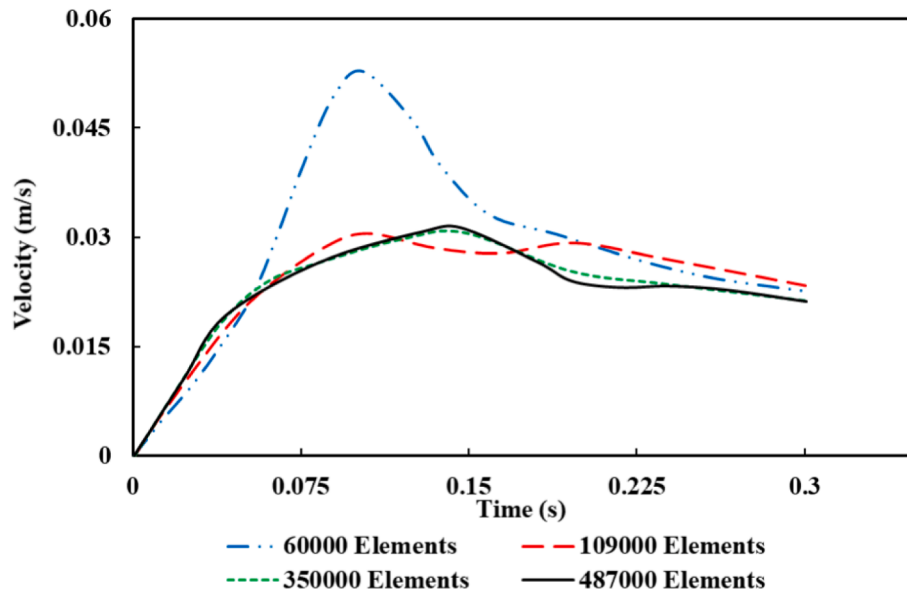
a
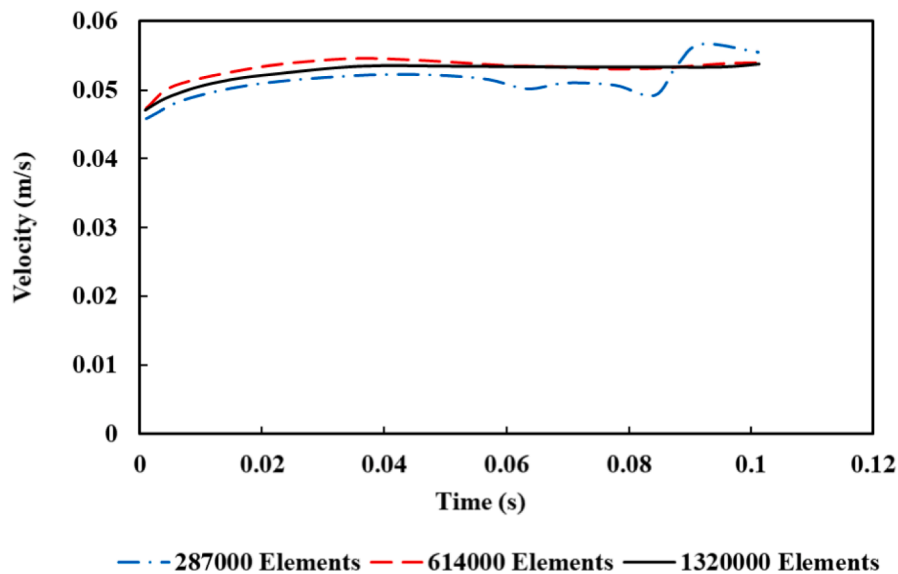
b

Fig. 4. Mesh independence assessment a. electro-coalescence b. microwave coalescence.

3. Results and discussion

3.1. Mesh sensitivity study

The assessment of the impact of the model mesh density on the output parameter is essential in ensuring that the solution is stable and shows minimal discretization errors. Hence, the grid independence study was conducted for the methods of coalescence utilized (Fig. 4). The mesh sensitivity analysis of the ultrasound coalescence was highlighted in a previous study [35]. Hence, fine mesh size of 101,434 was used for the ultrasound method. Four different mesh sizes namely coarse, base, fine and extremely fine meshes were examined for the electro-coalescence and microwave coalescence (Table 1). Courant numbers lower than one was set for the meshes to ensure model stability. This condition could be observed in different reports on water–oil multiphase flows [62,63]. Moreover, for accurate capture of the electromagnetic waves, a condition of mesh element size, $h \leq \frac{\lambda}{20}$, was utilized in agreement with the reports such as Litman et al. [64] and Malyuskin and Fusco [65]. However, further mesh refinement was required for the capture of the flow phenomena. The coarse mesh showed poor predictions of the flow velocity of the water droplets. The droplet velocity is an important contributor to settling, coalescence and separation. Although the estimations with the baseline meshes provide improvements over the coarse meshes, there were still significant mismatch over time. Hence, the fine meshes was used for further analysis of the electro-coalescence and microwave coalescence. The fine meshes require relatively less computational time, and provides close estimations within ~5% to the extremely fine meshes.

3.2. Model validation

The numerical model for the electro-coalescence was validated with the experimental study of Mohammadi et al. [66]. The work is based on the electro-coalescence of two water droplets in crude oil. The water has viscosity and dielectric constant of 0.97 mPa s and 1000, respectively. The crude oil has viscosity and dielectric constant of 15.1 mPa s and 2.5, respectively. The properties of the water and crude oil is presented in Table 2. The experiments consist of two electrodes, one on the left with high voltage and the other on the right with ground voltage. The high voltage was obtained from a signal generator with frequency of 50 Hz and sinusoidal voltage amplitude of 10–20 kV (Table 3). The mean radius of the binary water droplets is ~625 μm. Four different experimental runs were used for the evaluation of the numerical model (Fig. 5). The electro-coalescence model showed good agreement with the study of Mohammadi et al. [66]. The predicted droplets approach time was within ~10% from the experimental report. The duration for the droplets approach was taken as the time for two separate droplets to come into contact. The approach time for the droplets decreased with rising applied voltage. Conversely, lower inter-droplet skew angle and distance lead to enhanced approach of the droplets, with reduced time observed. The ultrasound model was validated in our previous report [35] with reasonable agreement with the work of Luo et al. [67]. The experimental study of Luo et al. [67] is based on the coalescence of water in white oil. Ultrasound frequency of 20 kHz and droplets radii of 137.5, 200 and 275 μm were assessed.

Table 1
Mesh types utilized for modeling the coalescence process.

Mesh Type	Number of Mesh Elements	
	Electro-coalescence	Microwave coalescence
Coarse	60,000	91,000
Base	109,000	287,000
Fine	350,000	614,000
Extremely Fine	487,000	1,320,000

Table 2
Properties of crude oil and water.

Fluid type	Viscosity (mPas)	Density (g/mL)	Dielectric constant	Surface tension (mN/m)
Crude oil	15.1	0.857	2.5	43
Water	0.97	1.020	1000	72

Table 3
Electro-coalescence conditions and droplets configuration [66].

No.	Preliminary inter-droplet skew (°) angle/distance (μm)	Droplets Radii (μm)	Mean electric field (kV/mm)	Applied voltage (kV)
1	3/452	616/624	28	20
2	6/668	618/625	28	20
3	19/462	605/625	28	20
4	2/506	618/625	14	10
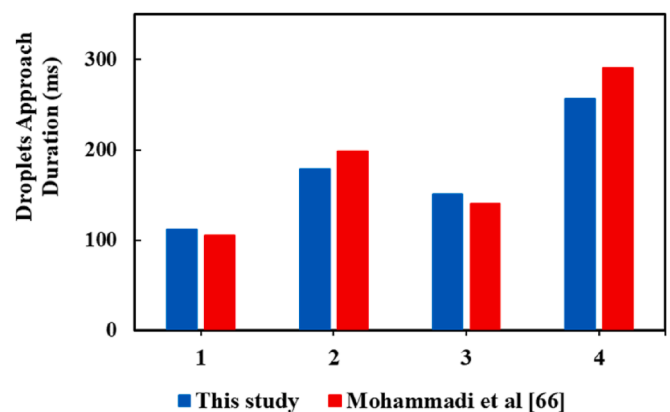
Fig. 5. Model validation with the electro-coalescence experiment of Mohammadi et al. [66].

3.3. Coalescence dynamics and energy assessment

The coalescence dynamics and energy assessment during the dehydration of two water droplets in crude oil was examined. The technical performance was analyzed based on the impact of varying inlet flow velocity, interfacial tension and viscosity of crude oil on the coalescence. The study of the coalescence dynamics allows for the determination of the demulsification parameters such as the droplets approach and coalescence times. Whilst the approach time signifies the time taken for two distant droplets to come into contact, the coalescence time is defined as the time it takes for the droplets to merge into a single droplet. These time estimations are strong indications of the dewatering efficiencies of crude oil emulsions. Moreover, the evaluation of the energy usage of the coalescence methods is critical because it influences the viability of large-scale implementations and process economics. This provides important information on the most effective methods for various operating conditions and emulsion properties.

3.3.1. Inlet flow velocity

The effect of the emulsion flow velocity on the coalescence dynamics and energy consumption was assessed for the three dehydration methods (Fig. 6). This is important for emulsion separation under continuous or semi-batch oil operations. Flow velocities between 10 and 100 mm/s were evaluated. The flow corresponds to the laminar region with Reynolds number (Re) of 40.74–407.36. There were significant differences between the coalescence time and energy usage for the methods studied. Generally, the process time of the dewatering process
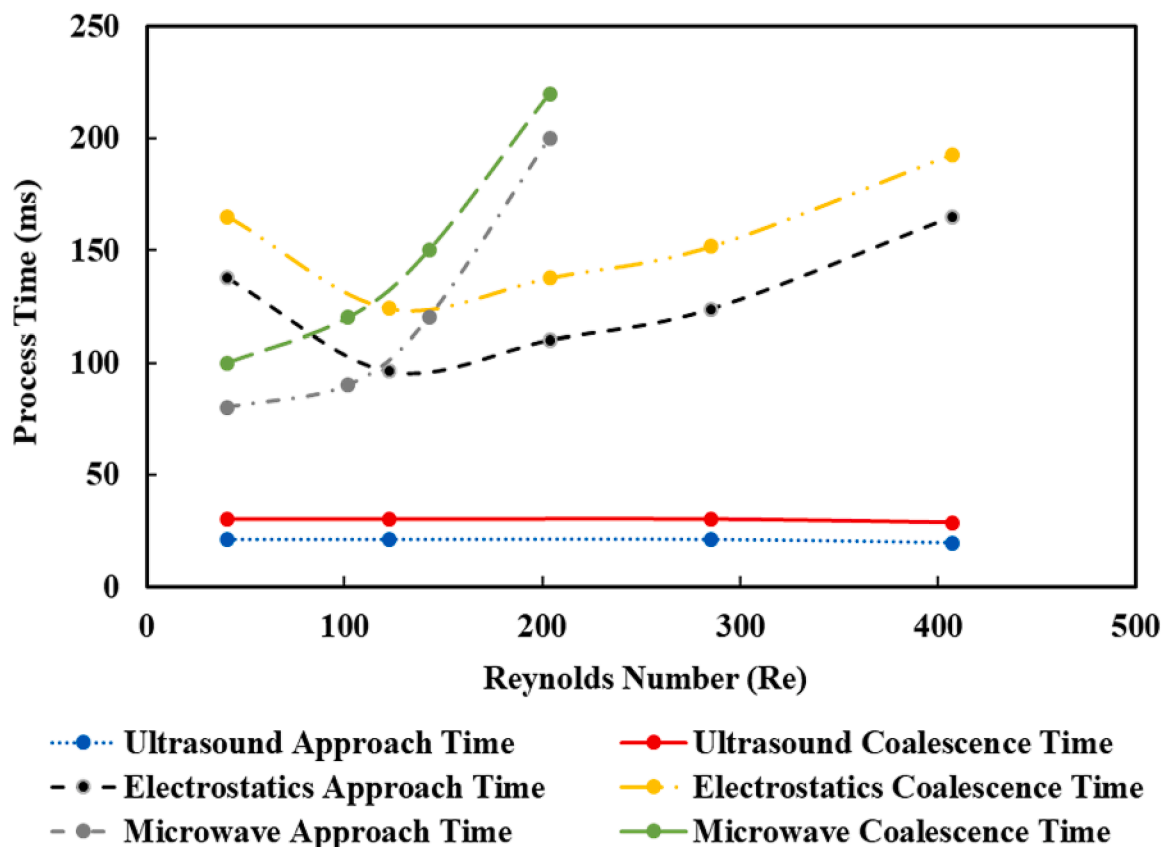
Fig. 6. Effect of inlet flow velocity on approach and coalescence time.

increased with rising inlet flow velocities. The behavior of the model in this manner is consistent with the experimental reports of microwave coalescence [20], ultrasound coalescence [68] and electro-coalescence [45,69]. For instance, Aterhortua [68] reported the lowering of the ultrasound demulsification efficiency of crude oil emulsion with 30 wt% water content as the flow velocity was elevated. Ultrasound of frequency of 1 MHz and combined power of 80 W was utilized. On increasing the emulsion flow rate from 50 to 100 mL/min, they highlighted that the unseparated water rose from 2.6 to 5.0 wt%. Similar observation was reported by Binner et al. [70] in their microwave demulsification experiments. For applied microwave power between 2 and 12 kW, the dehydration time increased consistently as the flow rate rose from 100 to 200 cm^3/s. The increasing trend of the coalescence time with velocity can be attributed to the increasing effect of flow disturbance and lowered residence time. In their study, Arnold and Stewart [71] noted that the residence time is influential on the coalescence process according to the following equation:

$$t = \frac{\pi}{6}\left(\frac{d_f{}^n - d_i{}^n}{\emptyset L_s}\right)$$

where d_f is the final droplet diameter, d_i is the starting droplet diameter, $\emptyset$ dispersed phase volume fraction, L_s is the definite system experimental parameter and n is the parameter indicating the probability of droplets bouncing prior to coalescence.

Flow fluctuations and reduced residence time could provide hindrance to the coalescence dynamics at higher velocities. This is demonstrated in the reduced final droplet size at lower residence times. At Re below 122.21, the coalescence time followed the order ultrasound < microwave < electrostatic supported coalescence. However, the order was ultrasound < electrostatics < microwave coalescence at Re above 122.21. The variation in the sequence with velocities can be attributed to the steeper rate of increase of the microwave coalescence time

relative to electro-coalescence. Furthermore, there was a reducing-increasing trend for electro-coalescence which transitions at about 30 mm/s. Ultrasound provides a consistent significant difference in comparison to microwave and electro-coalescence. Microwave and electro-coalescence showed close process time at flow velocity of ~30 mm/s. For instance, the coalescence time was 25, 130, 130 ms for ultrasound, electrostatics and microwave enhanced coalescence. However, the difference in the performance of electro-coalescence and microwave coalescence becomes wider at velocities farther from 30 mm/s. Whilst microwave provides improved performance over electro-coalescence by a margin of 70 ms at 10 mm/s, electro-coalescence showed enhancement of 90 ms at 50 mm/s. The performance of coalescence at higher velocities could be bolstered by the utilization of flow straighteners, avoidance and minimization of chokes and valves in regions of demulsification and the integration of ultrasound with microwave or electrostatics techniques.

Likewise, the flow velocity of the crude oil emulsion impacts the energy usage during dewatering processes (Fig. 7). The energy usage followed the order ultrasound < microwave < electrostatics coalescence methods at Re lower than 81.48. Whilst lower energy yielded faster coalescence with ultrasound, more energy was consumed to achieve a relatively slower coalescence with microwave and electric field enhancement. For example, at 10 mm/s, coalescence times of 30.00, 165.08, and 100.00 ms were attained with energies of 30x10^{-3}, 32.06 and 25.4 J for ultrasound, electrostatics and microwave techniques, respectively. Conversely, the sequence at Re more than 81.48 was ultrasound < electrostatics < microwave. Hence, ultrasound provides the best performance in terms of coalescence performance and energy usage at all flow velocities investigated.

3.3.2. Viscosity

The influence of crude oil viscosity on the coalescence of the binary
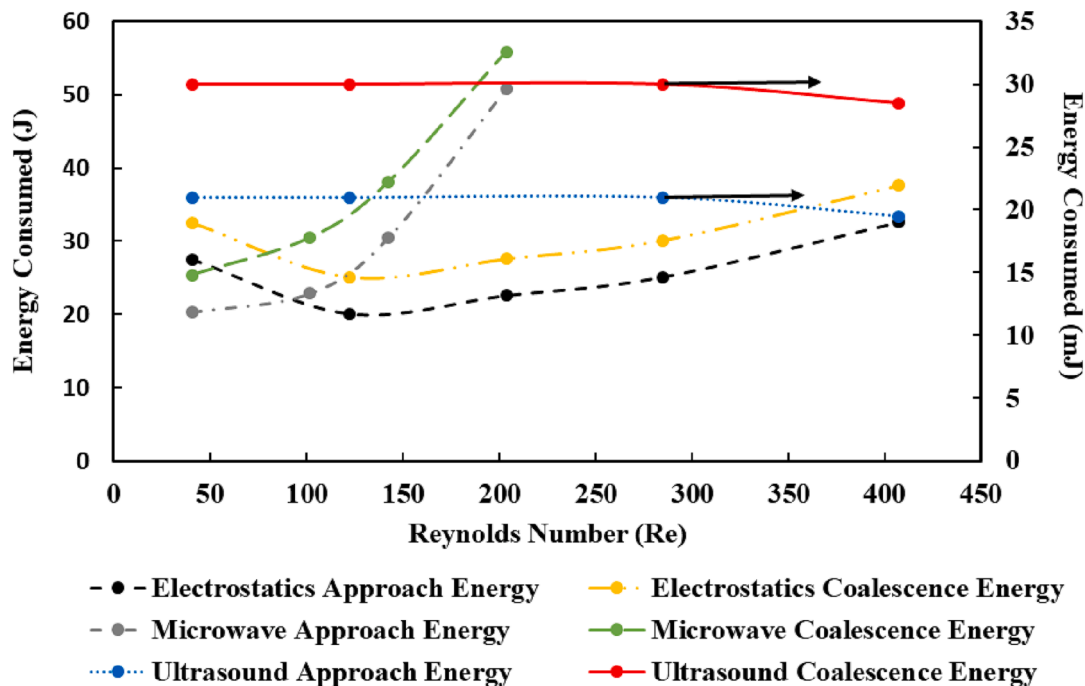
Fig. 7. Effect of inlet flow velocity on energy consumption.

water droplets at 10–106 mPa s was examined. This range allows for the investigation of broad types of crude oil. The viscosity showed significant impact on the coalescence of the water droplets. Generally, the process time for the droplets coalescence and approach increased as the Re decreased and viscosity increased for the approaches studied (Fig. 8). This behavior could be associated with the inhibition of flow dynamics at increased viscosities. Moreover, there are reports of attenuation of ultrasound as the fluid viscosity is elevated [72–74]. The process time followed the order ultrasound < electrostatics < microwave coalescence. The difference between the coalescence and approach times are ~7.4, ~21 and ~32 ms for ultrasound, electrostatics and microwave techniques, respectively. There are indications from experimental reports in the literature that support this sequence of coalescence time [75–81]. For instance, Yang et al. [76] observed that sono-chemical methods produced enhanced crude oil dewatering over thermal-

chemical coalescence approach. They reported demulsification efficiencies of 48.2 and 79.2% at 55 °C for thermal and ultrasound assisted methods, respectively, under similar crude oil emulsion properties. Furthermore, the coalescence time and demulsification efficiency outlined for electrostatics method is usually significantly more than those of ultrasound techniques at different viscosities. Yin et al. [80] highlighted that the coalescence of two water droplets in oil resulted in increased approach time with viscosity. The approach time increased from 1050 ms to 4450 ms as the oil viscosity was raised from 29.5 to 96.2 mPa s. In the study of Huang et al. [75], the approach and coalescence time obtained for coalescence under electric field were 770 and 848 ms, respectively. The electric field, droplet diameter, oil viscosity was 5.4×10^5 V/m, 0.6 mm and 870 mPa s, respectively. In a different work, Huang et al. [78] showed that the coalescence was attained after 117 ms for a less viscous silicone oil (viscosity = 20.47 mPa s) under AC field of
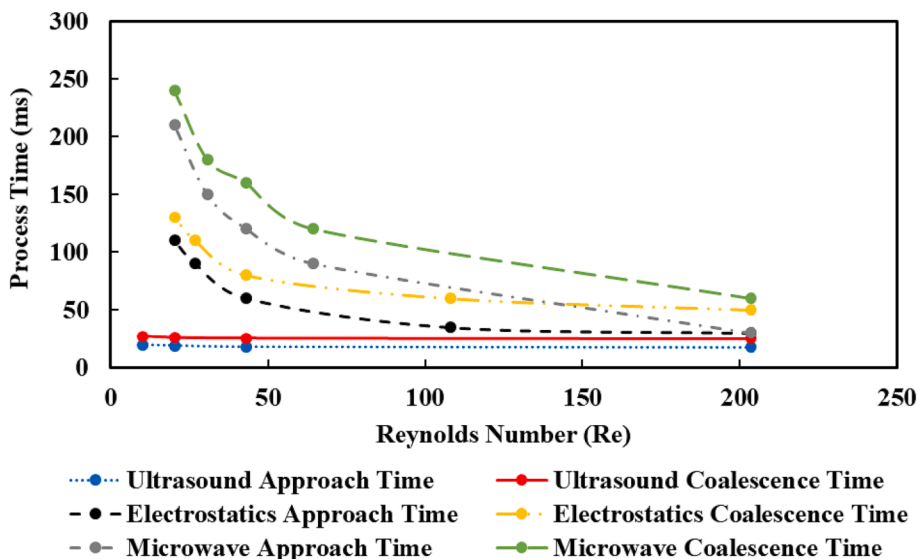
Fig. 8. Effect of crude oil viscosity on approach and coalescence time.

3.75×10^5 V/m. This is significantly higher in comparison to ultrasonic approaches [33,67]. Luo et al. [67] showed that the coalescence of binary droplets provided coalescence times of ~20 and ~30 ms with viscosity increment from 791 mPa to 1410 mPa s.

The energy consumption decreased as the Re was increased for the three coalescence approaches assessed (Fig. 9). This can be attributed to the lower crude oil viscosity requirements at higher Re. As the coalescence time is delayed due to flow inhibition and attenuation, more energy would be consumed for the emulsion separation at lower Re. Furthermore, the coalescence energy increased from ~15 J, ~90 J and ~25 mJ to ~61 J, ~235 J and ~26 mJ for microwave, electrostatics and ultrasound techniques, respectively, as the viscosity was raised from 10.6 to 106 mPa s. The order of performance of the methods is ultrasound < microwave < electrostatics. Although microwave coalescence requires more process time, lower energy was utilized in comparison to electro-coalescence. For instance, whilst the coalescence times was ~250 and ~130 ms for microwave and electrostatics, the energy usage was ~240 and ~53 J, respectively, at 106 mPa s. Ultrasound coalescence showed significant energy savings in comparison to microwave and electro-coalescence. The coalescence time and energy consumption are ~26 ms and ~26 mJ, respectively. Hence, ultrasound coalescence would be a potential method for standalone or integrated demulsification. However, Parvasi et al. [49] mentioned that ultrasound performance reduced significantly for high viscous oils. They highlighted that microwave showed enhanced separation than ultrasound coalescence beyond a certain viscosity limit. Luo et al. [34] have indicated that this limit is above 300 mPa s. Beyond this viscosity, the impact of ultrasound becomes weak with significant hindrance to droplet movement and accumulation.

3.3.3. Interfacial tension

The impact of the IFT between water and oil on coalescence time and energy usage was examined at 25–250 mN/m (Figs. 10 and 11). The values were selected because they represent similar range of IFT that have been reported in the literature [35]. Generally, the coalescence time increased as the Weber number (We) was increased. This can be associated with the improved stability of emulsions formed at reduced IFT under rising We. At lower IFT, the droplet restorative stress exceeds the external stress. The restorative stresses include the droplet surface stress and droplet internal viscous stress. Based on the force balance, Hinze [82] described the peak diameter that could be sustained by droplets as follows:

$$d_{peak} = We_{cr}^{\frac{3}{5}} \left(\frac{\sigma}{\rho_o} \right)^{3/5} \varepsilon^{-2/5}$$

where σ is the interfacial tension, ε is the average rate of energy dissipation, ρ_o is the crude oil density, We_{cr} is the critical Weber number.

Hence, lowering the IFT reduces the maximum size of the droplets that are attainable in the emulsion. Moreover, the coalescence followed the order ultrasound < microwave < electrostatics approaches. The improvements in the coalescence time for the microwave over electrostatics could be attributed to changes in the fluid properties with selective heating. Due to temperature gradient between the oil and water, the IFT and viscosity is lowered. The IFT is lowered more by the expansion of the droplet volume because of the microwave heating. Consequently, coalescence is enhanced by elevated frequency of collision and lowered flow inhibition [20].

The energy usage increased with rising We for all the coalescence approaches (Fig. 11). The energy consumption followed the sequence of ultrasound < electrostatics < microwave for IFTs lower than 140 mN/m. However, the order of energy utilization was ultrasound < microwave < electrostatics for IFT more than 140 mN/m. Ultrasound consistently showed the least energy requirement amongst the three methods evaluated. For instance, the energy consumption reduced from ~12 mJ to ~7.5 mJ as the IFT increased from 25 to 250 mN/m. In contrast, microwave and electrostatics methods consumed ~8 J and ~12 J at 250 mN/m. In addition, it could be observed that microwave was more effective in saving energy when the IFT is less than 140 mN/m.

3.4. Economic analysis

Based on the technical performance of the coalescence methods, the cost estimation was determined at different oil flow velocities (Fig. 12 a-b). Three conditions including cases 1, 2 and 3 were evaluated. Case 1 has a Re of 40.74 and flow velocity of 10 mm/s; case 2 has a Re of 122.21 and flow velocity of 30 mm/s; and case 3 has a Re of 203.68 and flow velocity of 50 mm/s. This provides the cost variations as the crude oil flow conditions are changed. The cost of energy of 6.27 cents per kWh, based on Dubai Electricity and Water Authority (DEWA) data, was utilized [83]. In addition, the cost of pumping was neglected in the economic assessment because the coalescence operation was assumed to be added on to an online crude oil processing and transportation plant. It
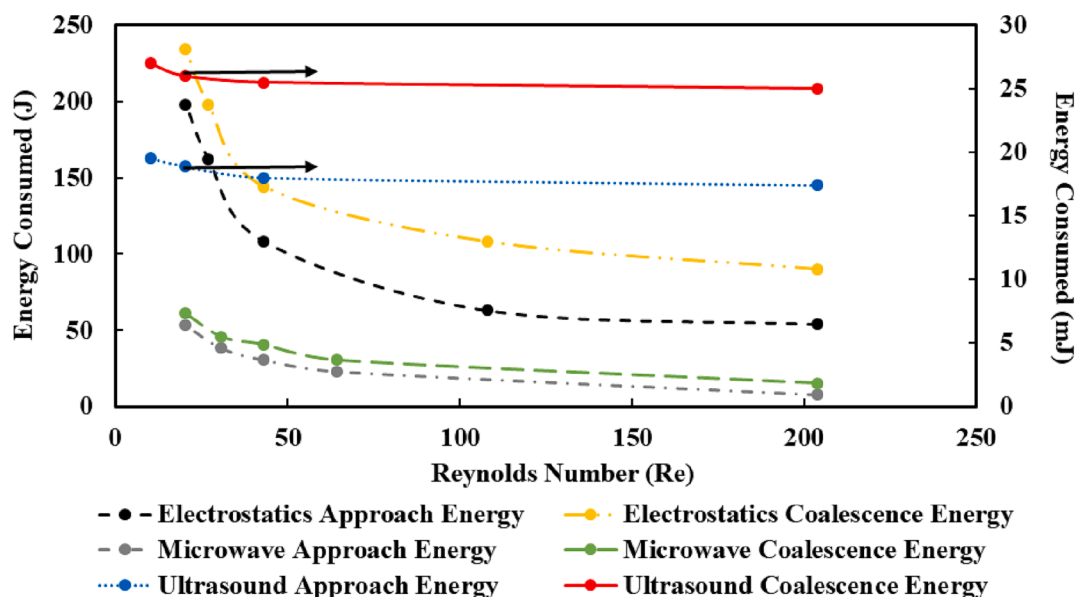
Fig. 9. Effect of crude oil viscosity on energy consumption.
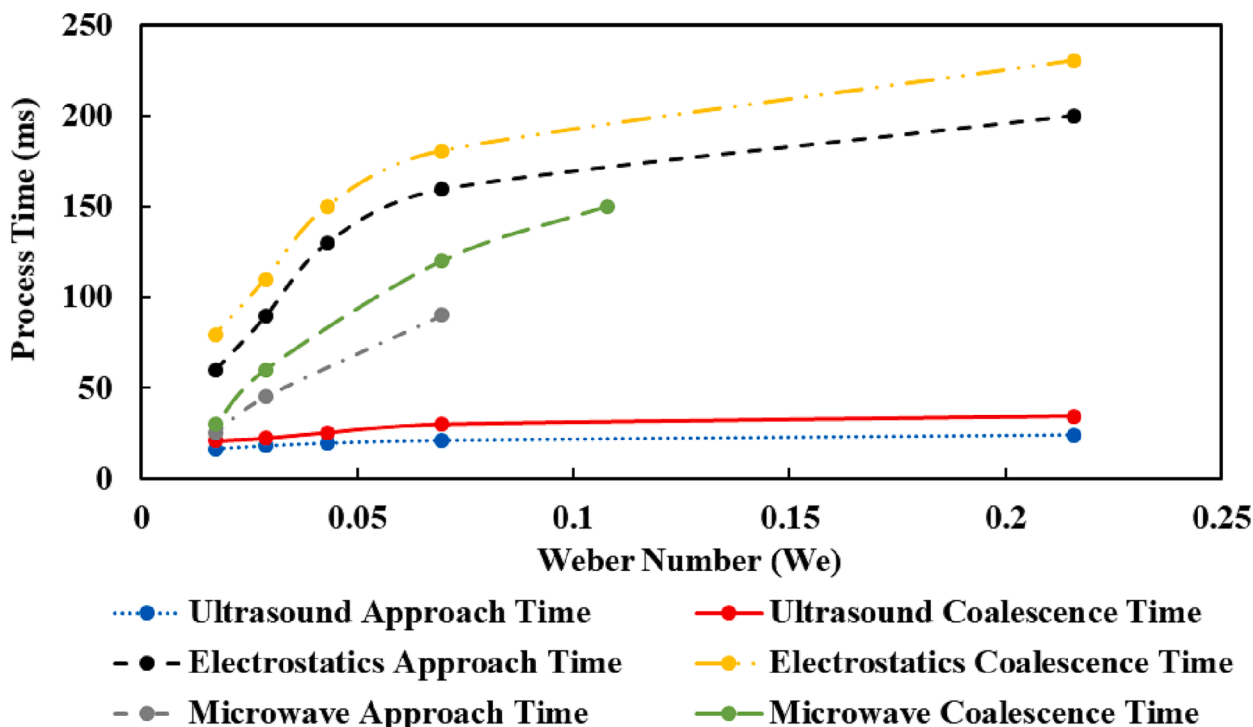
Fig. 10. Effect of interfacial tension on approach and coalescence time.
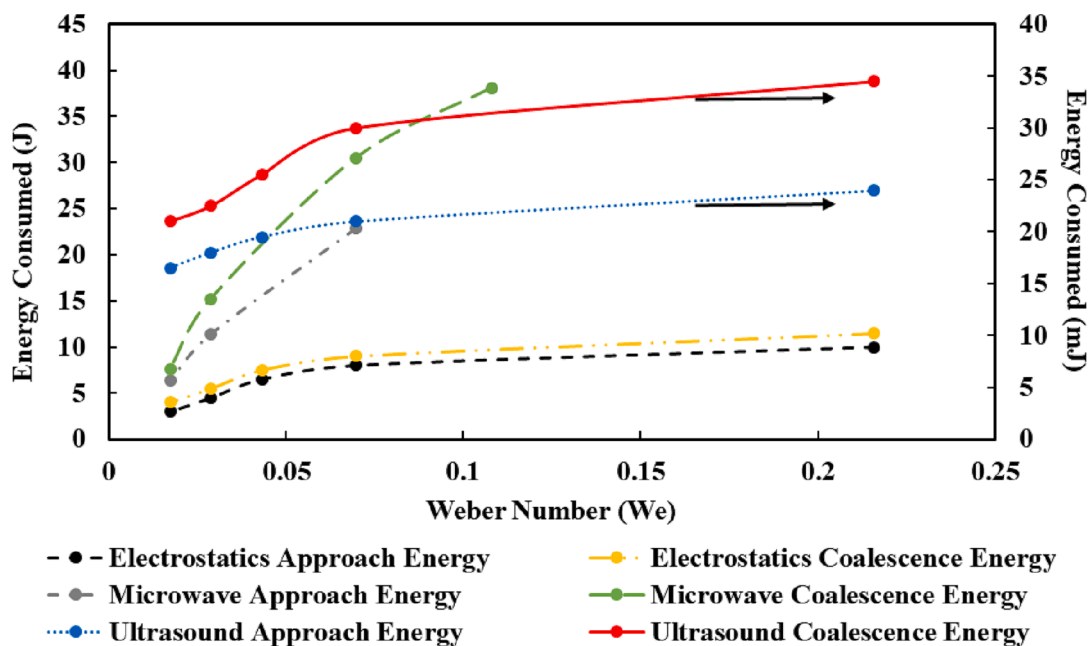
Fig. 11. Effect of interfacial tension on energy consumption.

could be observed that the unit annual price of coalescence of the two droplets with ultrasound was $ 32.92 at the different flow velocities. The unit yearly cost of coalescence with electric field increased from $ 6499 to $ 6590.98 as the flow velocity was elevated from 10 to 50 mm/s, respectively. Microwave coalescence exhibited higher cost than electrostatic assisted coalescence except at 30 mm/s. The unit annual cost rose from $ 6698.25 to $ 7603.04 as the emulsion velocity increased from 10 to 50 mm/s. The unit costs of the coalescence of the binary droplets could be extended to industrial and commercial scale demulsification through scaling estimates. For instance, different studies such

as Leister et al. [84], Hamedani [86] and Boxall et al. [85] have outlined some coalescence scaling methods.

4. Conclusion

In this study, the comparative assessment of the technical performance, energy usage and economic analysis of ultrasound, electrostatic and microwave enhanced coalescence of binary water droplets in crude oil was conducted numerically. The effect of different oil properties and operation conditions on the coalescence time and energy consumption
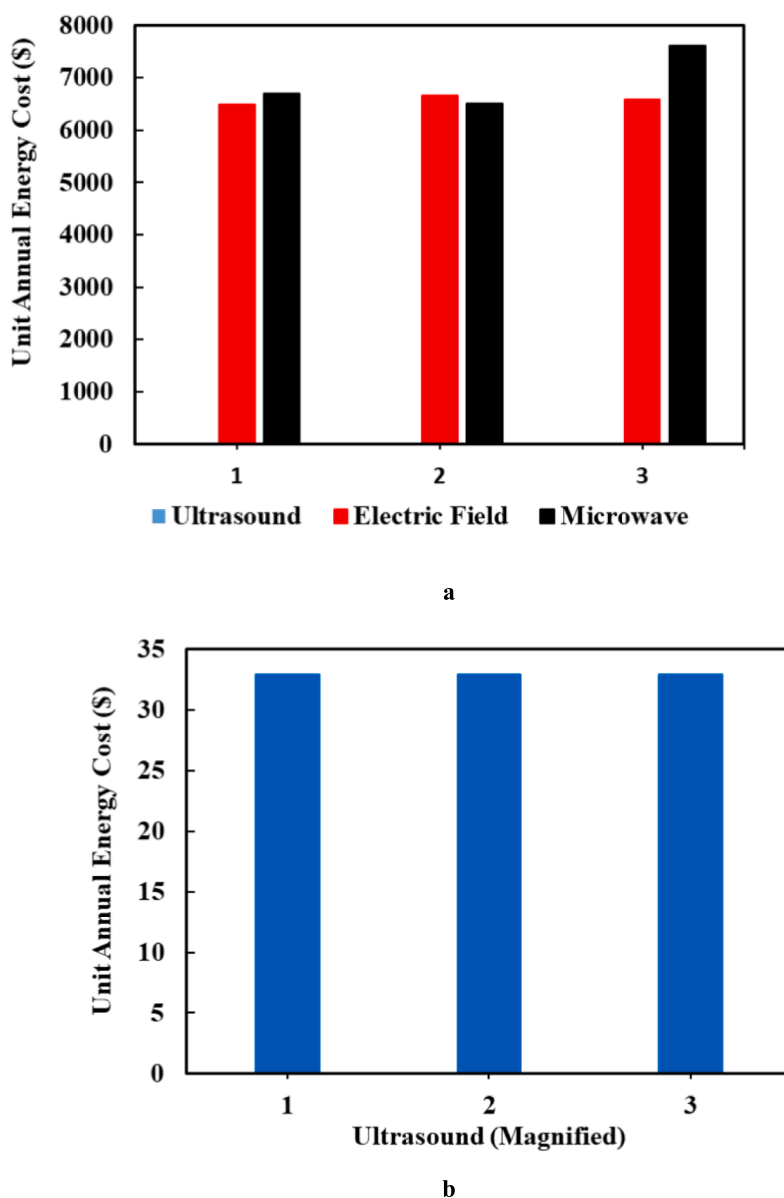
Fig. 12. Effect of inlet flow velocity on the process economics a. ultrasound, electric field and microwave enhanced coalescence b. ultrasound (magnified).

was examined. The numerical coalescence model showed good agreement with experimental findings in the literature. Moreover, the process time of the dewatering process increased with rising inlet flow velocities. The increasing trend of the coalescence time with velocity can be attributed to the intensification of the flow disturbance, and the reduction in the residence time of the emulsion. The behavior of the model in this manner is consistent with the experimental reports of microwave coalescence, ultrasound coalescence and electro-coalescence. As regards the IFT, the coalescence time reduced as the IFT was increased. This can be associated with the improved stability of emulsions formed at reduced IFT. At lower IFT, the droplet restorative stress exceeds the external stress. The restorative stresses include the droplet surface stress and droplet internal viscous stress. Based on the force balance, Hinze [82] described the peak diameter that could be sustained by droplets. As the maximum droplet size is directly proportional to the IFT, lowering the IFT reduces the peak diameter of the droplets that are present in the emulsion. Moreover, the coalescence

time followed the order ultrasound < microwave < electrostatics approaches under varying IFT.

The coalescence energy increased from ~15 J, ~90 J and ~25 mJ to ~61 J, ~235 J and ~26 mJ for microwave, electrostatics and ultrasound techniques, respectively, as the viscosity was raised from 10.6 to 106 mPa s. Ultrasound coalescence showed significant energy and economic savings in comparison to microwave and electro-coalescence. Hence, ultrasound coalescence would be a potential method for standalone or integrated demulsification over the two other techniques. However, Parvasi et al. [49] mentioned that ultrasound performance reduced significantly for very high viscous oils. They highlighted that microwave showed enhanced separation than ultrasound coalescence at elevated oil viscosity. Luo et al. [34] have indicated that this behavior occurs at viscosities above 300 mPa s. Beyond this viscosity, the impact of ultrasound becomes weak with significant hindrance to droplet movement and accumulation. The parameters of the coalescence of the binary droplets could be extended to industrial and commercial scale

demulsification through scaling estimates. For instance, different studies such as Leister et al. [84], Hamedani [86] and Boxall et al. [85] have outlined some coalescence scaling methods. This analysis provides fundamental insights on the behavior of the three emulsion separation techniques under similar emulsion properties and process condition.

CRediT authorship contribution statement

Idowu Adeyemi: Formal analysis, Methodology, Software, Writing – original draft, Writing – review & editing. **Mahmoud Meribout:** Conceptualization, Methodology, Writing – review & editing. **Lyes Khezzar:** Conceptualization, Methodology, Writing – review & editing. **Nabil Kharoua:** Methodology, Writing – review & editing. **Khalid AlHammadi:** Conceptualization, Methodology.

Declaration of Competing Interest

The authors declare that they have no known competing financial interests or personal relationships that could have appeared to influence the work reported in this paper.

Acknowledgement

References

[1] V.B. Guthrie, The raw material, crude petroleum and natural gas. Petroleum Products Handbook, first ed., McGraw-Hill, New York, 1960.

[2] J.S. Eow, M. Ghadiri, A.O. Sharif, T.J. Williams, Electrostatic enhancement of coalescence of water droplets in oil: a review of the current understanding, Chem. Eng. J. 84 (3) (2001) 173–192.

[3] R.W. Bryers, Fireside slagging, fouling, and high-temperature corrosion of heat-transfer surface due to impurities in steam-raising fuels, Prog. Energy Combust. Sci. 22 (1) (1996) 29–120.

[4] J.G. Speight, Handbook of petroleum product analysis, John Wiley & Sons, 2015.

[5] F.G. Antes, L.O. Diehl, J.S. Pereira, R.C. Guimarães, R.A. Guarnieri, B.M. Ferreira, E.M. Flores, Effect of ultrasonic frequency on separation of water from heavy crude oil emulsion using ultrasonic baths, Ultrason. Sonochem. 35 (2017) 541–546.

[6] H.J. Gary, G.E. Handwerk, Crude Distillation, Petroleum Refining-Technology and Economics, 2006.

[7] M.F. Pedrotti, M.S. Enders, L.S. Pereira, M.F. Mesko, E.M. Flores, C.A. Bizzi, Intensification of ultrasonic-assisted crude oil demulsification based on acoustic field distribution data, Ultrason. Sonochem. 40 (2018) 53–59.

[8] S. Kokal, M. Wingrove, Emulsion separation index: From laboratory to field case studies, in: SPE Annual Technical Conference and Exhibition. OnePetro.

[9] M.A. Saad, N.H. Abdurahman, R.M. Yunus, H.S. Ali, An overview of recent technique and the affecting parameters in the demulsification of crude oil emulsions, in: IOP Conference Series: Materials Science and Engineering, vol. 991, No. 1 (2020, December). IOP Publishing, p. 012105.

[10] X. Long, G. Zhang, C. Shen, G. Sun, R. Wang, L. Yin, Q. Meng, Application of rhamnolipid as a novel biodemulsifier for destabilizing waste crude oil, Bioresour. Technol. 131 (2013) 1–5.

[11] X. Long, N. He, Y. He, J. Jiang, T. Wu, Biosurfactant surfactin with pH-regulated emulsification activity for efficient oil separation when used as emulsifier, Bioresour. Technol. 241 (2017) 200–206.

[12] E. Yonguep, K.K. Fabrice, J.K. Katende, M. Chowdhury, Formation, stabilization and chemical demulsification of crude oil-in-water emulsions: A review, Petrol. Res. (2022).

[13] D. Wang, D. Yang, C. Huang, Y. Huang, D. Yang, H. Zhang, Q. Liu, T. Tang, M.G. El-Din, T. Kemppi, B. Perdicakis, Stabilization mechanism and chemical demulsification of water-in-oil and oil-in-water emulsions in petroleum industry: A review, Fuel 286 (2021), 119390.

[14] F. Mohammadi, H. Sanaeishoar, E. Tahanpesar, Application of a novel surface modified mesoporous silica nanoparticles as chemical demulsifiers for breaking water-in-crude oil emulsion, Pet. Sci. Technol. (2022) 1–18.

[15] A.O. Ezzat, A.M. Atta, H.A. Al-Lohedan, Demulsification of stable seawater/ Arabian heavy crude oil emulsions using star-like tricationic pyridinium ionic liquids, Fuel 304 (2021) 121436.

[16] N.A. Kakhki, M. Farsi, M.R. Rahimpour, Effect of current frequency on crude oil dehydration in an industrial electrostatic coalescer, J. Taiwan Inst. Chem. Eng. 67 (2016) 1–10.

[17] A. Sadatshojaie, D.A. Wood, S.M. Jokar, M.R. Rahimpour, Applying ultrasonic fields to separate water contained in medium-gravity crude oil emulsions and determining crude oil adhesion coefficients, Ultrason. Sonochem. 70 (2021), 105303.

[18] A.M. Sousa, M.J. Pereira, H.A. Matos, Oil-in-water and water-in-oil emulsions formation and demulsification, J. Pet. Sci. Eng. 110041 (2021).

[19] D. Santos, E.C. da Rocha, R.L. Santos, A.J. Cancelas, E. Franceschi, A.F. Santos, M. Fortuny, C. Dariva, Demulsification of water-in-crude oil emulsions using single mode and multimode microwave irradiation, Sep. Purif. Technol. 189 (2017) 347–356.

[20] E.R. Binner, J.P. Robinson, S.A. Silvester, S.W. Kingman, E.H. Lester, Investigation into the mechanisms by which microwave heating enhances separation of water-in-oil emulsions, Fuel 116 (2014) 516–521.

[21] H. Sabati, H. Motamedi, Efficient separation of water-in-oil petroleum emulsions by a newly isolated biodemulsifier producing bacterium, Delftia sp. strain HS3, Environ. Exp. Biol. 18 (2) (2020) 129–134.

[22] Q. Cai, Z. Zhu, B. Chen, B. Zhang, Oil-in-water emulsion breaking marine bacteria for demulsifying oily wastewater, Water Res. 149 (2019) 292–301.

[23] H. Sabati, H. Motamedi, Investigation of the relationship between cell surface hydrophobicity and demulsifying capability of biodemulsifier-producing bacteria, Front. Biol. 13 (5) (2018) 358–365.

[24] Q. Zhang, K.O. Vigier, S. Royer, F. Jerome, Deep eutectic solvents: synthesis, properties and applications, Chem. Soc. Rev. 41 (2012) 7108–7146.

[25] Z. Maugeri, P. Domínguez, Novel choline-chloride-based deep-eutectic-solvents with renewable hydrogen bond donors: levulinic acid and sugar-based polyols, RSC Adv. 2 (2012) 421–425.

[26] A.P. Abbott, G. Capper, D.L. Davies, R. Rasheed, Ionic liquid based metal halide/ substituted quaternary ammonium salt mixtures, Inorg. Chem. 43 (2004) 3447–3452.

[27] M. Sivapragasam, M. Moniruzzaman, M. Goto, An overview on the toxicological properties of ionic liquids toward microorganisms, Biotechnol. J. 15 (4) (2020) 1900073.

[28] J. Flieger, M. Flieger, Ionic liquids toxicity—benefits and threats, Int. J. Mol. Sci. 21 (17) (2020) 6267.

[29] W. Faisal, F. Almomani, A critical review of the development and demulsification processes applied for oil recovery from oil in water emulsions, Chemosphere 133099 (2021).

[30] S. Sonwani, S. Madaan, J. Arora, S. Suryanarayan, D. Rangra, N. Mongia, T. Vats, P. Saxena, Inhalation exposure to atmospheric nanoparticles and its associated impacts on human health: a review, Front. Sustain. Cities 3 (2021), 690444.

[31] X. Luo, H. Gong, Z. He, P. Zhang, L. He, Recent advances in applications of power ultrasound for petroleum industry, Ultrason. Sonochem. 70 (2021) 105337.

[32] I. Adeyemi, M. Meribout, L. Khezzar, Recent developments, challenges, and prospects of ultrasound-assisted oil technologies, Ultrason. Sonochem. 82 (2022), 105902.

[33] Z. Xu, Numerical simulation of the coalescence of two bubbles in an ultrasound field, Ultrason. Sonochem. 49 (2018) 277–282.

[34] X. Luo, H. Gong, J. Cao, H. Yin, Y. Yan, L. He, Enhanced separation of water-in-oil emulsions using ultrasonic standing waves, Chem. Eng. Sci. 203 (2019) 285–292.

[35] I. Adeyemi, M. Meribout, L. Khezzar, N. Kharoua, K. AlHammadi, Numerical assessment of ultrasound supported coalescence of water droplets in crude oil, Ultrason. Sonochem. 88 (2022), 106085.

[36] G.D. Pangu, D.L. Feke, Droplet transport and coalescence kinetics in emulsions subjected to acoustic fields, Ultrasonics 46 (4) (2007) 289–302.

[37] C. Lesaint, W.R. Glomm, L.E. Lundgaard, J. Sjöblom, Dehydration efficiency of AC electrical fields on water-in-model-oil emulsions, Colloids Surf. A Physicochem. Eng. Asp. 352 (1–3) (2009) 63–69.

[38] S. Less, A. Hannisdal, E. Bjørklund, J. Sjöblom, Electrostatic destabilization of water-in-crude oil emulsions: Application to a real case and evaluation of the Aibel VIEC technology, Fuel 87 (12) (2008) 2572–2581.

[39] P.P. Kothmire, Y.J. Bhalerao, V.M. Naik, R.M. Thaokar, V.A. Juvekar, Experimental studies on the performance and analysis of an electrostatic coalescer under different electrostatic boundary conditions, Chem. Eng. Res. Des. 154 (2020) 273–282.

[40] V. Vivacqua, S. Mhatre, M. Ghadiri, A.M. Abdullah, A. Hassanpour, M.J. Al-Marri, B. Azzopardi, B. Hewakandamby, B. Kermani, Electrocoalescence of water drop trains in oil under constant and pulsatile electric fields, Chem. Eng. Res. Des. 104 (2015) 658–668.

[41] X. Lv, Z. Song, J. Yu, Y. Su, X. Zhao, J. Sun, Y. Mao, W. Wang, Study on the demulsification of refinery oily sludge enhanced by microwave irradiation, Fuel 279 (2020), 118417.

[42] S. Akbari, A. Nour, S. Jamari, A. Rajabi, Demulsification of water-in-crude oil emulsion via conventional heating and microwave heating technology in their optimum conditions, Aust. J. Basic Appl. Sci. 10 (4) (2016) 66–74.

[43] L. Kovaleva, R. Zinnatullin, A. Musin, R. Gabdrafikov, R. Sultanguzhin, V. Kireev, Influence of radio-frequency and microwave electromagnetic treatment on water-in-oil emulsion separation, Colloids Surf. A Physicochem. Eng. Asp. 614 (2021), 126081.

[44] N.H. Abdurahman, R.M. Yunus, N.H. Azhari, N. Said, Z. Hassan, The potential of microwave heating in separating water-in-oil (w/o) emulsions, Energy Proc. 138 (2017) 1023–1028.

[45] T. Assenheimer, A. Barros, K. Kashefi, J.C. Pinto, F.W. Tavares, M. Nele, Evaluation of microwave and conventional heating for electrostatic treatment of a water-in-oil model emulsion in a pilot plant, Energy Fuel 31 (6) (2017) 6587–6597.

[46] R. Martínez-Palou, R. Cerón-Camacho, B. Chávez, A.A. Vallejo, D. Villanueva-Negrete, J. Castellanos, J. Karamath, J. Reyes, J. Aburto, Demulsification of heavy crude oil-in-water emulsions: A comparative study between microwave and thermal heating, Fuel 113 (2013) 407–414.

[47] X.G. Yang, W. Tan, X.F. Tan, Demulsification of crude oil emulsion via ultrasonic chemical method, Pet. Sci. Technol. 27 (17) (2009) 2010–2020.

[48] M. Yi, J. Huang, L. Wang, Research on crude oil demulsification using the combined method of ultrasound and chemical demulsifier, J. Chem. (2017).

[49] P. Parvasi, A.K. Hesamedini, A. Jahanmiri, M.R. Rahimpour, A comparative study on droplet coalescence in heavy crude oil emulsions subjected to microwave and ultrasonic fields, Sep. Sci. Technol. 48 (11) (2013) 1591–1601.

[50] H. Salah, A Novel Experimental Study of Crude Oil Dehydration Using Microwave Energy Under Electrostatic Field, 2019.

[51] H. Lu, Z. Pan, Z. Miao, X. Xu, S. Wu, Y. Liu, H. Wang, Q. Yang, Combination of electric field and medium coalescence for enhanced demulsification of oil-in-water emulsion, Chem. Eng. J. Adv. 6 (2021), 100103.

[52] H. Gong, W. Li, X. Zhang, Y. Peng, B. Yu, Y. Mou, Simulation of the coalescence and breakup of water-in-oil emulsion in a separation device strengthened by coupling electric and swirling centrifugal fields, Sep. Purif. Technol. 238 (2020), 116397.

[53] S.A. Issaka, Application of Microwave and Ultrasonic Demulsification Techniques on Petroleum Based Emulsions, (Doctoral dissertation, UMP), 2012.

[54] W. Tan, X.G. Yang, X.F. Tan, Study on demulsification of crude oil emulsions by microwave chemical method, Sep. Sci. Technol. 42 (6) (2007) 1367–1377.

[55] L. Xia, K. Gong, S. Wang, J. Li, D. Yang, Microwave-assisted chemical demulsification of water-in-crude-oil emulsions, J. Dispers. Sci. Technol. 31 (11) (2010) 1574–1578.

[56] A. Khajehesamedini, A. Sadatshojaie, P. Parvasi, M.R. Rahimpour, M. M. Naserimojarad, Experimental and theoretical study of crude oil pretreatment using low-frequency ultrasonic waves, Ultrason. Sonochem. 48 (2018) 383–395.

[57] X. Xu, D. Cao, J. Liu, J. Gao, X. Wang, Research on ultrasound-assisted demulsification/dehydration for crude oil, Ultrason. Sonochem. 57 (2019) 185–192.

[58] COMSOL, Acoustic module user's guide, 2021.

[59] COMSOL, AC/DC module user's guide, 2021.

[60] COMSOL, RF module user's guide, 2021.

[61] COMSOL, CFD module user's guide, 2021.

[62] M. Guilizzoni, G. Salvi, G. Sotgia, L.P.M. Colombo, Numerical simulation of oil-water two-phase flow in a horizontal duct with a Venturi flow meter, J. Phys.: Conf. Ser. 1224(1) (2019). IOP Publishing, p. 012008.

[63] H. Joshi, L. Dai, A numerical investigation on a flow of a viscous oil drop in water inside a small diameter capillary tube, in: ASME International Mechanical Engineering Congress and Exposition, vol. 45202, American Society of Mechanical Engineers, 2012, pp. 1047–1053.

[64] A. Litman, H. Tortel, M. Guillaume, Resolution-improved microwave tomography by means of hyperspectral analysis tools, in: Proceedings of the XIII Internarional Conference on Ground Penetrating Radar, IEEE, 2010, pp. 1–5.

[65] O. Malyuskin, V.F. Fusco, High-resolution microwave near-field surface imaging using resonance probes, IEEE Trans. Instrum. Meas. 65 (1) (2015) 189–200.

[66] M. Mohammadi, S. Shahhosseini, M. Bayat, Electrocoalescence of binary water droplets falling in oil: Experimental study, Chem. Eng. Res. Des. 92 (11) (2014) 2694–2704.

[67] X. Luo, J. Cao, L. He, H. Wang, H. Yan, Y. Qin, An experimental study on the coalescence process of binary droplets in oil under ultrasonic standing waves, Ultrason. Sonochem. 34 (2017) 839–846.

[68] C.M.G. Atehortúa, N. Pérez, M.A.B. Andrade, L.O.V. Pereira, J.C. Adamowski, Water-in-oil emulsions separation using an ultrasonic standing wave coalescence chamber, Ultrason. Sonochem. 57 (2019) 57–61.

[69] Y. Shi, J. Chen, H. Meng, Experimental study on the performance of an electric field enhanced separator for crude oil production fluid, J. Pet. Sci. Eng. 212 (2022), 110315.

[70] E.R. Binner, J.P. Robinson, S.W. Kingman, E.H. Lester, B.J. Azzopardi, G. Dimitrakis, J. Briggs, Separation of oil/water emulsions in continuous flow using microwave heating, Energy Fuel 27 (6) (2013) 3173–3178.

[71] K. Arnold, M. Stewart, Design of oil-handling systems and facilities, Gulf Professional Publishing, 1998.

[72] S. Majumdar, P.S. Kumar, A.B. Pandit, Effect of liquid-phase properties on ultrasound intensity and cavitational activity, Ultrason. Sonochem. 5 (3) (1998) 113–118.

[73] G.G. Stokes, On the theories of the internal friction of fluids in motion and of the equilibrium and motion of elastic solids, Trans. Cambridge Philos. Soc. 8 (1845) (1845) 287–319.

[74] V.A. Shutilov, M.E. Alferieff, Fundamental physics of ultrasound, CRC Press, 2020.

[75] X. Huang, L. He, X. Luo, H. Yin, D. Yang, Deformation and coalescence of water droplets in viscous fluid under a direct current electric field, Int. J. Multiph. Flow 118 (2019) 1–9.

[76] D. Yang, Y. Sun, L. He, X. Luo, Y. Lü, Coalescence characteristics of droplets at oil–water interface subjected to different electric waveforms, Chem. Eng. Process.-Process Intensification 134 (2018) 28–37.

[77] X. Luo, H. Yin, H. Yan, X. Huang, D. Yang, L. He, The electrocoalescence behavior of surfactant-laden droplet pairs in oil under a DC electric field, Chem. Eng. Sci. 191 (2018) 350–357.

[78] X. Huang, L. He, X. Luo, K. Xu, Y. Lü, D. Yang, Convergence effect of droplet coalescence under AC and pulsed DC electric fields, Int. J. Multiph. Flow 143 (2021), 103776.

[79] X. Luo, J. Cao, H. Yan, H. Gong, H. Yin, L. He, Study on separation characteristics of water in oil (W/O) emulsion under ultrasonic standing wave field, Chem. Eng. Process.-Process Intensification 123 (2018) 214–220.

[80] H. Yin, X. Luo, K. Xu, H. Yan, L. He, Electrocoalescence kinetics of binary droplets in a viscous fluid, Chem. Eng. Sci. 224 (2020), 115788.

[81] K. Guo, Y. Lv, L. He, X. Luo, D. Yang, Experimental study on the dehydration performance of synergistic effect of electric field and magnetic field, Chem. Eng. Process.-Process Intensification 142 (2019), 107555.

[82] J.O. Hinze, Fundamentals of the hydrodynamic mechanism of splitting in dispersion processes, AIChE J 1 (3) (1955) 289–295.

[83] W.M. Taqqali, N. Abdulaziz, Smart grid and demand response technology, in: 2010 IEEE International Energy Conference, IEEE, 2010, pp. 710–715.

[84] N. Leister, C. Yan, H.P. Karbstein, Oil Droplet Coalescence in W/O/W Double Emulsions Examined in Models from Micrometer-to Millimeter-Sized Droplets, Colloids Interfaces 6 (1) (2022) 12.

[85] J.A. Boxall, C.A. Koh, E.D. Sloan, A.K. Sum, D.T. Wu, Droplet size scaling of water-in-oil emulsions under turbulent flow, Langmuir 28 (1) (2012) 104–110.

[86] B. Khadem-Hamedani, Design, Scale-up and Optimization of Double Emulsion Processes (Doctoral dissertation, Lyon), 2019.

[87] I.N. Evdokimov, A.P. Losev, Microwave treatment of crude oil emulsions: Effects of water content, J. Pet. Sci. Eng. 115 (2014) 24–30.